ACS Sustainable Chemistry & Engineering

Research Article

Cite This: ACS Sustainable Chem. Eng. 2018, 6, 17368−17375

pubs.acs.org/journal/ascecg

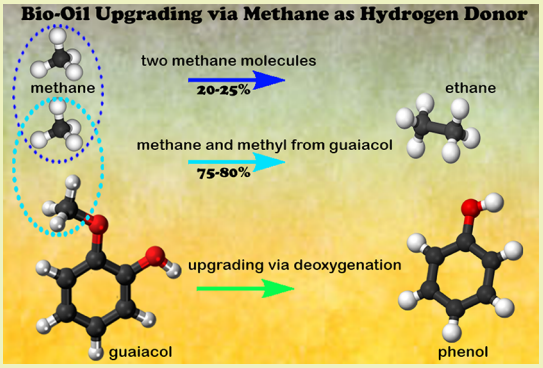
Bio-Oil Upgrading Using Methane: A Mechanistic Study of Reactions of Model Compound Guaiacol over Pt−Bi Bimetallic Catalysts

Yang Xiao and Arvind Varma*

Davidson School of Chemical Engineering, Purdue University, 480 Stadium Mall Drive, West Lafayette, Indiana 47907, United States

Supporting Information

ABSTRACT: Biomass and shale/natural gas will be two important alternative resources for fuel and chemical production for at least the next century. Bio-oil, deriving from the fast pyrolysis of lignin, is a key second generation biofuel, containing high oxygen content. Hydrodeoxygenation (HDO) is typically employed to improve the quality of bio-oils, while the high cost of hydrogen prevents its commercialization. On the other hand, although it is the primary component of shale and natural gas, methane direct conversion to higher hydrocarbons has remained a challenge since the 1980s. Following our recent work, in the present study, methane is used to upgrade guaiacol, a well-known model compound of bio-oils, over Pt−Bi bimetallic catalysts supported on activated carbon (AC). Various characterization techniques, including transmission electron microscopy (TEM), X-ray diffraction (XRD), Brunauer−Emmett−Teller (BET), H_2 temperature-programmed desorption (H_2-TPD), H_2−O_2 titration, inductively coupled plasma atomic emission spectroscopy (ICP-AES), temperature−programmed oxidation (TPO) and temperature−programmed surface reaction (TPSR), were utilized to obtain catalyst structure and properties. It was found that as compared to the Pt catalyst, Pt−Bi bimetallic catalysts exhibited relatively stable (no significant deactivation) guaiacol upgrading performance for 8 h TOS (time on stream), generating partially deoxygenated products along with ethane. The addition of Bi suppresses coke formation, improving catalyst stability. The isotopic labeling tests demonstrate that ethane is produced either from coupling of two methane molecules (20−25%) or from a methane molecule combining with a methyl from guaiacol (75−80%).



KEYWORDS: *Bio-oil upgrading, Shale and natural gas utilization, Methane coupling, Pt−Bi bimetallic catalysts, Isotopic labeling, Improving catalyst stability*

Downloaded via PURDUE UNIV on December 3, 2018 at 21:52:03 (UTC).
See https://pubs.acs.org/sharingguidelines for options on how to legitimately share published articles.

INTRODUCTION

Biomass conversion to renewable fuels has received increasing attention in recent years, which has the potential to improve the overall profitability from agricultural/forest resources in the U.S. and reduce emissions of greenhouse gas (GHG) globally.[1−3] First generation biofuels (e.g., ethanol and biodiesel) cause concern regarding high food prices, which can be addressed by utilization of nonfood crop feedstocks, leading to second generation biofuels. As a nonfood crop component, lignin is abundant and the only biomass constituent based on aromatic units, contributing approximately 30% of the weight and 40% of the energy content of lignocellulosic biomass.[4] To efficiently convert lignin, fast pyrolysis is a promising approach, producing bio-oils that contain significantly higher oxygen content as compared to traditional petroleum-derived oils.[5,6] Therefore, owing to their characteristics such as thermal instability, corrosiveness, poor volatility, high coking tendency, and low heating value, bio-oils cannot be directly used as engine fuels.[7,8] To improve the quality of bio-oils to meet fuel specifications, upgrading via catalytic hydrodeoxygenation (HDO) is typically followed,[9−11] in which hydrogen plays a key role as reductant. The high cost ($2500/ton) of H_2 from various sources, including electrolysis, natural gas reforming and coal gasification; however, limits commercialization of bio-oil upgrading processes, although extensive HDO research has been widely carried out.[12−14]

Methane is the main component (~70−95%) of natural and shale gas. The efficient conversion of methane to higher hydrocarbons (C_{2+}) and oxygenated chemicals (e.g., methanol, formaldehyde) provides attractive routes for production of alternative energy and chemicals.[15,16] A well-known methane direct conversion is oxidative coupling of methane (OCM), producing C_2 species (ethane/ethylene). It remains a long-standing challenge for decades, owing to the difficulty in tuning methane selectivity toward target products under oxidative conditions.[17] Nonoxidative conversion of methane, producing C_2−C_8 hydrocarbons, has been reported since 1993,[18] which typically achieves relatively high selectivity toward higher hydrocarbons.[19] In our recent report,[20] highly selective nonoxidative coupling of methane over Pt−Bi bimetallic catalysts was presented, achieving >90% carbon selectivity toward C_2 species. Nonoxidative

Received: September 25, 2018
Published: October 23, 2018

© 2018 American Chemical Society

DOI: 10.1021/acssuschemeng.8b04925
ACS Sustainable Chem. Eng. 2018, 6, 17368−17375

methane conversion is, however, limited by thermodynamic equilibrium conversion (0.5−8% at 600−700 °C), and catalyst stability issues arise at higher temperatures owing to coke formation.[21]

To develop a cheaper reductant instead of hydrogen for bio-oil upgrading as well as efficiently utilizing shale and natural gas, as reported in our prior investigation,[22] methane ($150/ton) was used to upgrade guaiacol ($C_7H_8O_2$)—a model compound of bio-oil. As partially deoxygenated species, the target products are phenol (C_6H_6O) and cyclopentanone (C_5H_8O) in the liquid phase, which are useful as chemicals, e.g. phenol as precursor to plastics and cyclopentanone as precursor to fragrances. It was found that when Pt−Bi bimetallic catalysts were employed, methane functioned as well as hydrogen for upgrading guaiacol. The promoter Bi was proposed as a site blocker over the Pt surface, leading to suppression of coke formation, as reported in the literature as well.[23−25] The use of guaiacol (2-methoxyphenol) as the model compound is justifiable since during bio-oil production, guaiacol-like species are typically formed by thermal degradation of lignin[26] and their concentration in the oil-phase can be as high as 34 wt % depending on the pyrolysis conditions.[27] Moreover, the two different oxygenated functions present in guaiacol, phenolic (Ph−OH) and methoxy (−OCH_3) groups, represent a large number of oxygen-containing components in lignin-derived bio-oils, such as eugenol and vanillin.[28] In our recent study,[29] kinetic investigations of liquid products (catechol, phenol, and cyclopentanone) were conducted. It was found that the model-predicted values such as guaiacol conversion and liquid product yields matched experimental measurements well. In addition to our prior works, Gunawardena et al. and He et al. utilized methane as a hydrogen source to upgrade bio-oil as well.[30−32]

In both of our prior studies,[22,29] excess methane (CH_4:guaiacol molar ratio = 10) was employed to achieve high guaiacol conversion over the 5% Pt−1% Bi/AC catalyst and ethane was always coproduced in the gas phase along with deoxgenated liquid phase products, indicating methane coupling to C_2 species. Effects of the methane/guaiacol feed ratio, Bi loading and the origin of carbon atom source in ethane, however, were not studied previously. To address these issues, in the present work, a mechanistic study of guaiacol deoxygenation using methane over various Pt−Bi bimetallic catalysts was carried out, including catalyst characterization, methane feed control experiments, correlation of gas-phase species partial pressures, and isotope labeling tests. Insights into methane/guaiacol feed ratio, Bi loading, and ethane formation pathway were obtained and discussed.

EXPERIMENTAL SECTION

Using $H_2PtCl_6(H_2O)_6$ and $BiCl_3$ as precursors, and 80−120 mesh activated carbon (AC) as support, Pt and Bi were sequentially loaded using the wet impregnation method. The catalysts were dried at 373 K in air before use. These catalysts were characterized by BET (Brunauer−Emmett−Teller), H_2-TPD (temperature-programmed desorption), TPSR (temperature-programmed surface reaction), H_2−O_2 titration, ICP-AES (inductively coupled plasma atomic emission spectroscopy), TEM (transmission electron microscopy), and powder XRD (X-ray diffraction) techniques.

The catalytic performance tests were conducted in a fixed-bed reactor setup, as described in our prior work.[33,22] Prior to reaction, the packed catalyst was activated at 400 °C and 1 atm for 4 h under a gas mixture flow (H_2:N_2 = 1:2). The reactor was then purged using N_2 for 30 min. The following standard operating conditions were used: 400 °C, 1 atm total pressure, 0.02−0.05 g catalyst for differential reactions (conversions typically <8%) and 0.5 g catalyst for integral reactions (conversions typically >10%), total gas (CH_4:N_2 = 1:1) flow rate 100 mL/min, and guaiacol feed rate 0.025 mL/min (liquid, at room temperature). The feed flow rates correspond to a molar ratio of 10 between CH_4 and guaiacol.

Differential/integral reactions were performed by varying packed amount of catalysts, leading to different guaiacol/methane conversions and partial pressure changes of gas-phase products. For isotopic labeling, $^{13}CH_4$ was cofed with guaiacol instead of normal $^{12}CH_4$, while products were analyzed by a mass spectrometry instrument. The mass balance of ^{13}C atoms was 97 ± 1%. Blank tests of AC support with no metal loading were conducted under the standard reaction conditions, and guaiacol conversion was less than 0.5%. Without guaiacol, methane exhibited less that 0.2% conversion, generating H_2 and trace C_2H_6 on Pt−Bi catalyst under the standard conditions. On the other hand, without methane, guaiacol exhibited less that 0.05% conversion. All experiments have carbon mass balances, including both liquid and gas phases, of 92 ± 2%, similar to the literature.[32,34,35] Unless stated otherwise, all data sets were taken at 10 min time on stream (TOS) as initial reaction rates. More detailed description of the experimental procedure, including materials, catalyst preparation, characterization, and product analysis, is provided in the Supporting Information (SI).

RESULTS AND DISCUSSION

Characterization Results. Five catalytic materials supported on activated carbon (AC), denoted as 5% Pt, 5% Pt−1% Bi, 5% Pt−2.5% Bi, 5% Pt−5% Bi, and 1% Bi, were prepared, characterized, and tested in the present study (see the SI—Materials and Catalyst Preparation). Note that the former two materials were also used in our prior work.[22] As shown in Table 1, all five materials exhibited high surface areas

Table 1. BET Characterization Results of Various Catalytic Materials

catalyst	BET surface area, m^2/g	pore size, nm	pore volume, cm^3/g
5% Pt	618	3.9	2.1
5% Pt−1% Bi	593	4.2	1.9
5% Pt−2.5% Bi	589	3.6	1.4
5% Pt−5% Bi	541	3.8	1.5
1% Bi	522	3.1	0.9
used 5% Pt	349	1.6	0.8
used 5% Pt−1% Bi	561	4.0	1.7

(520−620 m^2/g), pore sizes in the range 3.1−4.2 nm, and pore volumes 0.9−2.1 cm^3/g, which were consistent with our prior report and the literature.[36,37] The elemental analysis of these materials is shown in Table 2. For fresh catalysts, both metal

Table 2. ICP-AES Element Analysis of Various Catalytic Materials

catalyst	Pt % (fresh)	Bi % (fresh)	Pt % (used)	Bi % (used)
5% Pt	4.7		4.7	
5% Pt−1% Bi	4.5	0.9	4.4	0.8
5% Pt−2.5% Bi	4.9	2.3	4.8	2.3
5% Pt−5% Bi	4.8	4.7	4.6	4.5
1% Bi		0.8		0.7

(Pt and Bi) compositions were essentially consistent as designed values, while for used catalysts, 2−4 wt % loss of both metals was found. This unavoidable metal leaching has been reported in the literature, although it is smaller here than prior reported values which were for liquid phase reaction.[38,39]

DOI: 10.1021/acssuschemeng.8b04925
ACS Sustainable Chem. Eng. 2018, 6, 17368−17375

The XRD patterns of all five catalysts exhibited no significant peaks in the range 5−90°, which is likely because of the relatively high Pt metal dispersions (~20−30%) and the amorphous structure of AC.[36,40−42] The TEM scans of four materials are shown in Figure S1, which indicates that metals (dark dots) were successfully loaded on the support and metal particle size was relatively small (typically 2−4 nm). Table 3 shows that

Table 3. TEM, H_2−O_2 Titration, and Turnover Frequency (TOF) of Various Catalytic Materials

	particle size, nm			
catalyst	TEM	H_2−O_2 titration	Pt dispersion, %	TOF, s^{-1}
5% Pt	3.4	4.2	22.0	0.119
5% Pt−1% Bi	3.0	3.9	29.3	0.078
5% Pt−2.5% Bi	2.7	3.3	24.2	0.081
5% Pt−5% Bi	2.6	3.1	23.5	0.049
1% Bi	4.3			
used 5% Pt		6.1	15.2	0.009
used 5% Pt−1% Bi		4.2	27.3	0.074

Pt dispersion values were in the range 20−30%, corresponding to Pt particle sizes 3.1−4.2 nm (based on H_2−O_2 titration[43]), which are consistent with the data from TEM scans (Figures S1 and S2).

Effect of Methane to Guaiacol Feed Ratio. Under standard operating conditions in the present work as well as our prior work,[22] the molar ratio of methane to guaiacol feed is 10:1. Owing to excess methane, the contribution of methane to reaction rate was considered as constant.[29] To investigate methane feed effect, in the present section, the ratio was varied in the range of 1 to 10. As shown in Figure 1, when the methane:guaiacol molar feed ratio was 1, negligible guaiacol conversion was observed, which was similar to the case without methane feed (see the Experimental Section). While when methane/guaiacol molar ratio was 2−4, guaiacol exhibited ~2−25% conversion, producing catechol (nondeoxygenated species) as the primary component. When the ratio was in the range 6−10, guaiacol reached essentially the same conversion (~ 90%), producing all three components (catechol, phenol and cyclopentanone) with stable selectivity values. These observations indicate that excess methane (e.g., methane:guaiacol molar ratio 6−10) gives good deoxygenation performance for guaiacol upgrading.

Effect of Bismuth Loading. In our prior work,[22] 1% Bi was added in 5% Pt, leading to the 5% Pt−1% Bi catalyst, which exhibited stable guaiacol deoxygenation performance using methane as reductant. To investigate bismuth addition effect, bismuth loadings were varied in the range 1−5%. Under standard operating conditions using methane as a reductant, the initial (TOS = 10 min, see the Experimental Section) liquid product compositions and guaiacol conversions over various Pt−Bi bimetallic catalysts are shown in Figure 2a. Note that the 1% Bi catalyst (without Pt presence) did not exhibit any guaiacol conversion (<0.5%), thus is not shown. Over all other four catalysts, catechol, phenol, and cyclopentanone were detected with relatively similar product distributions (see Figure 2a for initial, i.e., TOS = 10 min, product distribution, and Figure S3 for stable product distributions over TOS = 0−8 h). As noted above, phenol and cyclopentanone, as valuable partially deoxygenated species, are the target products in the present work. Over the 5% Pt catalyst, guaiacol conversion was 90.1% with the lowest Pt dispersion (22%) and highest turnover frequency (TOF) value (0.119 s^{-1}) (see Table 3). Guaiacol conversions over 5% Pt−1% Bi, 5% Pt−2.5% Bi, and 5% Pt−5% Bi were 78.9%, 68.0%, and 60.4%, respectively, following a decreasing trend with more Bi addition. This is likely in part owing to the decrease of Pt dispersion (29.3%, 24.2%, and 23.5%) as shown in Table 3. When compared to pure Pt catalyst, Bi addition improves Pt dispersion values (from 22% to 24−29%), while it gives lower TOF values (0.049−0.081 s^{-1}). This suggests that Bi addition blocks some Pt surface atoms from functioning as active sites for guaiacol and/or methane activation.[20,44] As shown in Figure 2b as well as in our prior work,[22] the 5% Pt catalyst was deactivated in less than 2 h TOS, although it showed the highest initial activity, while all the other three Pt−Bi bimetallic catalysts exhibited relatively good stability over the investigated period (TOS = 8 h).

In Figure 3a, H_2 temperature-programmed desorption (H_2-TPD) profiles for various Pt−Bi catalysts demonstrate that hydrogen adsorption/desorption decreased with Bi addition

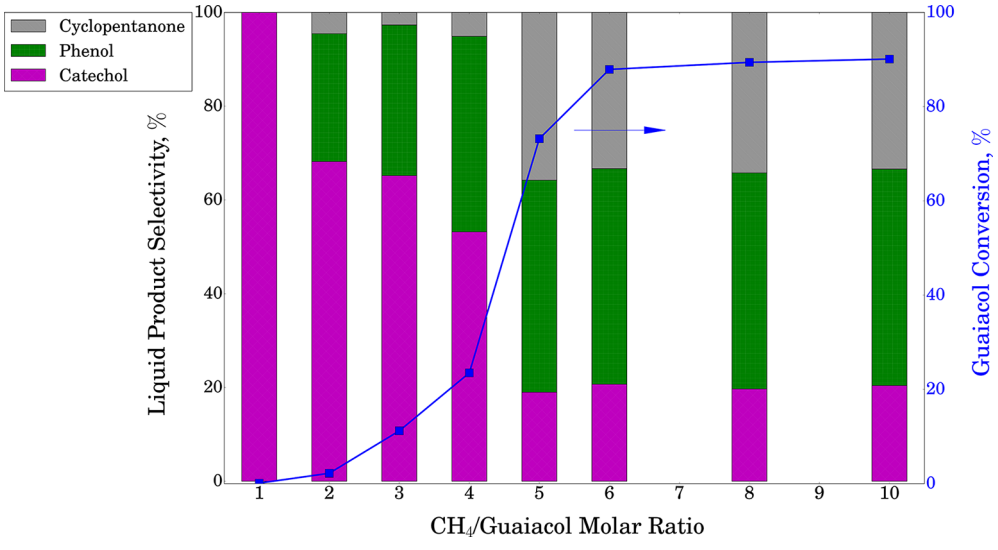


Figure 1. Effect of methane to guaiacol feed ratio over the 5% Pt−1% Bi catalyst: 400 °C, 1 atm, 0.5 g catalyst, total gas flow 100 mL/min with CH_4:N_2 = 1:1, guaiacol liquid feed rate 0.025 mL/min, TOS = 10 min.

DOI: 10.1021/acssuschemeng.8b04925
ACS Sustainable Chem. Eng. 2018, 6, 17368−17375

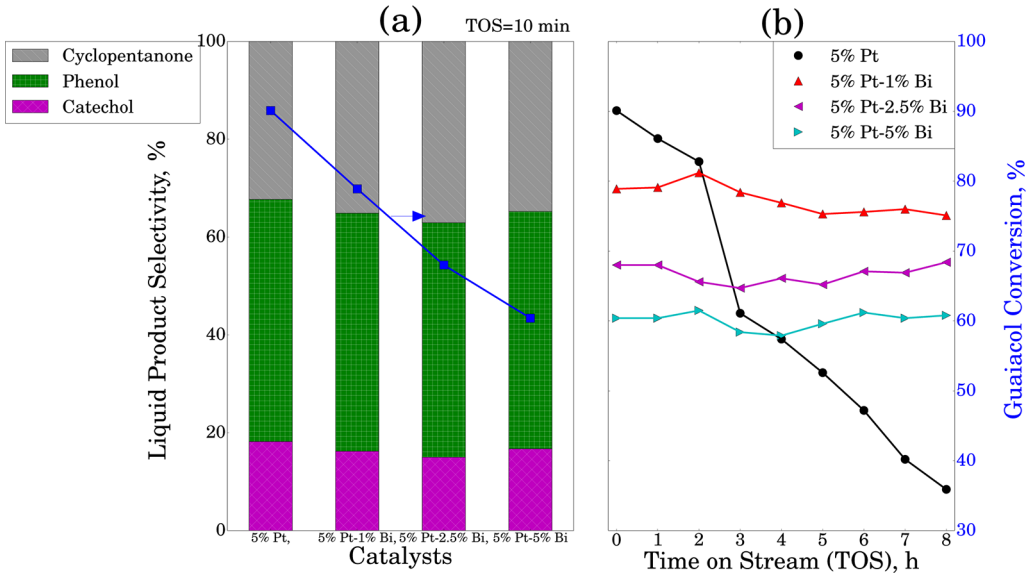


Figure 2. Effect of bismuth loading for (a) liquid product selectivity at TOS = 10 min and (b) catalyst stability within TOS = 8 h: 400 °C, 1 atm, 0.5 g catalyst, total gas flow 100 mL/min with CH_4:N_2 = 1:1, guaiacol liquid feed rate 0.025 mL/min.

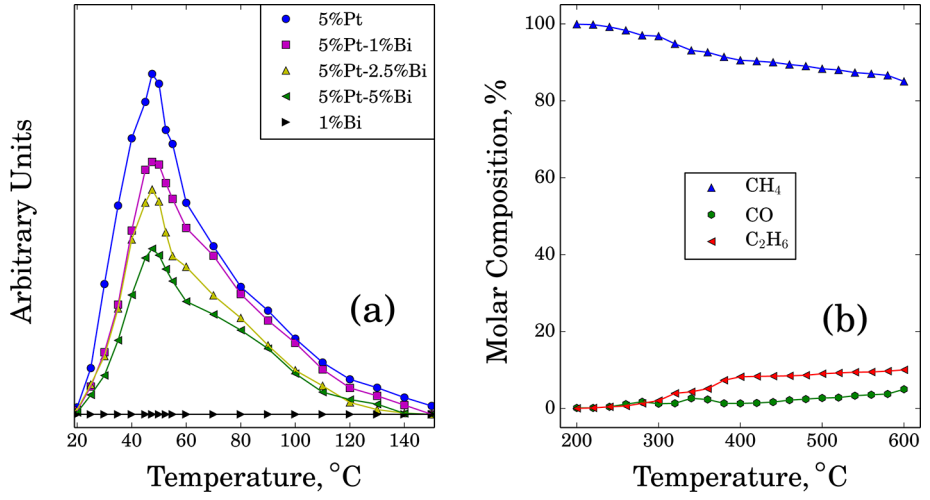


Figure 3. Temperature-programmed investigations: (a) H_2 desorption (H_2-TPD) from different Pt−Bi catalysts and (b) surface reaction (TPSR) profiles over the 5% Pt−1% Bi catalyst.

increase to the 5% Pt catalyst, corresponding to lowering Pt active sites and suppressed coke formation.[45,46] Figures 3a and 2b, taken together, show that Bi addition to Pt improves catalyst stability via suppressing coke formation by blocking some Pt surface sites. For 1% Bi catalyst, no significant hydrogen adsorption was observed, indicating the inactive nature for the pure Bi catalyst. These observations are consistent with the above discussion on the basis of Figure 2a and b. In Figure 3b, temperature-programmed surface reaction (TPSR) profiles show that, below 300 °C, guaiacol and methane cannot be efficiently activated, owing to the chemical stability of methane and guaiacol molecules. Between ca. 300 to 450 °C, methane was consumed, producing both CO and C_2H_6 in the gas phase. From ca. 450 to 550 °C, methane conversion along with CO and C_2H_6 yields continued to increase, while the yield of liquid products decreased, as reported in our prior study.[22] In addition, similar CH_4-TPD experiments were carried out. Note that in the TPD procedure (see the SI−Catalyst Characterization), gas adsorption is first performed at room temperature (20 °C), followed by desorption under programmed temperature. It was found that no notable CH_4 adsorption occurred at room temperature. This indicates that CH_4 does not adsorb over Pt or Pt−Bi catalysts at room temperature. Thus the CH_4-TPD profile is not shown in the present work.

BET and H_2−O_2 titration measurements were also performed for used 5% Pt and 5% Pt−1% Bi catalysts, and the results are shown in Tables 1 and 3, respectively. As compared with fresh catalysts, the surface area, pore size, pore volume, metal dispersion, and TOF values of used 5% Pt decreased, while its particle size (determined by H_2−O_2 titration) increased, indicating metal particle sintering. On the other hand, for the 5% Pt−1% Bi catalyst, all of these values, including particle size, were not changed significantly. In addition, Figure S4a and b shows temperature-programmed oxidation (TPO) profiles for used 5% Pt and 5% Pt−1% Bi catalysts, respectively. Initial oxidation of used 5% Pt started at ca. 320 °C, followed by two large peaks at 450 and 550 °C and a smaller peak at 580 °C (also see Table S1). For used 5% Pt−1% Bi, however, only

DOI: 10.1021/acssuschemeng.8b04925
ACS Sustainable Chem. Eng. 2018, 6, 17368−17375

two distinguished peaks at 440 and 560 °C were identified. By integrating curves in Figure S4, accumulated coke amounts were obtained and are listed in Table S1. The used 5% Pt−1% Bi contained much less coke (40 mg/g_{cat}) than the used 5% Pt (546 mg/g_{cat}), which is considered as the key factor for better stability as shown in Figure 2b. The TPO profiles suggest that by adding Bi to Pt catalysts, coke formation was suppressed when methane was used as a reductant for guaiacol deoxygenation reaction,[23] although guaiacol conversion was decreased slightly, likely owing to the less active nature of Pt−Bi as compared to pure Pt catalysts.[46]

Carbon Source of Gas-Phase Products: Isotopic Labeling for Ethane and CO Formation Pathways. As proposed in our prior works,[22,29] reaction pathways in Figure 4

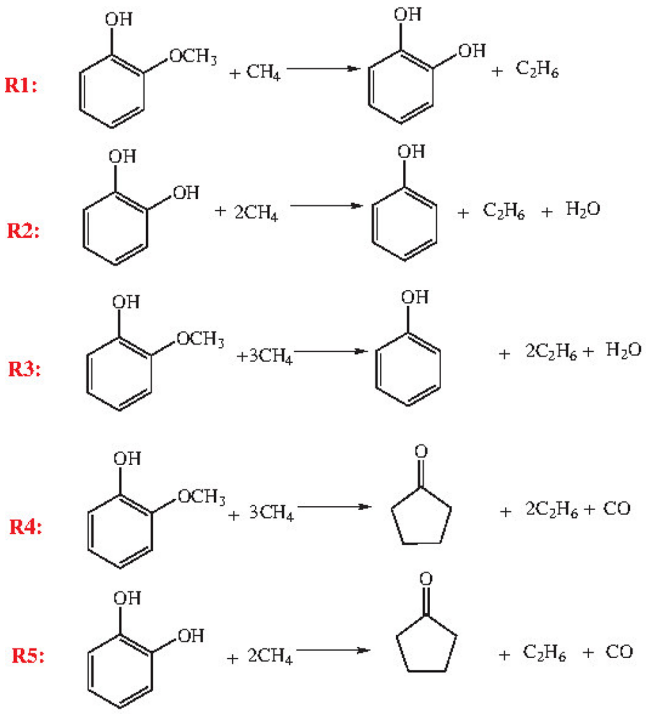


Figure 4. Reaction pathways for guaiacol deoxygenation network using methane.

describe the network of guaiacol deoxygenation, while the carbon source (i.e., guaiacol and/or methane) of gas-phase products (i.e., ethane and CO) remains unclear. Note that steps R1−R5 in Figure 4 are not proposed as elementary reactions. All experiments for this figure were carried out under the same feed flow rates of both methane and guaiacol, while the packed amounts of catalyst were varied. Both differential/integral reactions were carried out via packing different amounts of catalyst, and isotope labeling experiments were also conducted.

Differential Reactions. To study the carbon source of gas-phase products, it is important to analyze steps R1−R5 in Figure 4 individually. Under integral operating conditions (e.g., guaiacol conversion >10%), however, all five steps (R1−R5) become significant, making it difficult to investigate individual steps. For this reason, differential operating conditions (guaiacol conversion less than 8%) were first applied. As noted in our prior work,[29] when using guaiacol as the feed under differential operating conditions, catechol is the only detectable product in the liquid phase, i.e. only step R1 in Figure 4 prevails while steps R3 and R4 are negligible. In this case, steps R2 and R5 are also negligible owing low concentration of catechol, the reactant for these two steps. This is likely due to lower reaction rates,[29] hence lower yields (smaller than 6−8%) of steps R3 and R4, as compared to step R1. Instead of guaiacol, when catechol is used as feed, also under differential conditions, both phenol and cyclopentanone (corresponding to steps R2 and R5) exist in the liquid products. Therefore, by using differential operating conditions, steps R1 and R2/R5 can be investigated separately.

As discussed above, to investigate step R1, guaiacol and methane were cofed under differential operating conditions over the 5% Pt−1% Bi catalyst and various methane conversion and gas-phase product (ethane and CO) yield values were obtained by varying catalyst packing weights. The partial pressure changes of methane and gas-phase products are plotted and correlated in Figure 5, where, as shown in part a, only one product (ethane) was found in the gas phase. The linear fit of methane and ethane partial pressure changes gives slope = −0.91, as defined by eq 1 below, which indicates that, in general, 1 mol C_2H_6 is formed when 1 mol CH_4 is consumed.

$$k = \frac{\Delta P_{C_2H_6}}{\Delta P_{CH_4}} \quad (1)$$

Further, isotope labeling experiments revealed that $^{12}CH_3-^{13}CH_3$ accounted for 98.93% of formed ethane (1.05% $^{13}CH_3-^{13}CH_3$ and negligible $^{12}CH_3-^{12}CH_3$). The above experimental observations clearly demonstrate that when step R1 in Figure 4 occurs, ethane is formed from a methane molecule combining with a methyl from guaiacol.

To investigate step R2 and R5, catechol and methane were cofed under differential operating conditions over the 5% Pt−1% Bi catalyst. Figure 5b was obtained by varying catalyst packing weights, similar to Figure 5a. It appears that both ethane and CO were produced by steps R2 and R5, which is consistent with the pathways presented in Figure 4. The partial pressure changes of both ethane and CO correlated well with methane partial pressure change, resulting in slopes −0.44 and −0.21, respectively. This implies that when steps R2 and R5 occurs simultaneously, when one mole ethane is formed, approximately 2 mol methane are consumed. Isotope labeling experiments additionally show that almost all formed ethane is $^{13}CH_3-^{13}CH_3$ (>99.5%), indicating methane coupling. Since no ^{13}CO (less than 0.01%) was detected, it appears that all CO was from catechol decomposition, which has been noted previously.[47] Note that the difference of slope values in Figure 5b likely owes to different rates of steps R2 and R5, since only step R5 produced CO, while both steps generated ethane.

Integral Reaction. To understand the origin of ethane when guaiacol conversion was greater than 10%, integral operating conditions were applied. By varying packed catalyst mass in a wider range, up to 90% guaiacol conversion was reached. Similar to Figure 5, partial pressure changes, in broader ranges, of gas-phase products and methane over the 5% Pt−1% Bi catalyst are plotted and correlated in Figure 6. It appears that the ratio of ethane formation to methane consumption is 0.86, close to the stoichiometric coefficient of step R1, indicating that step R1 dominates when all five steps (R1−R5) occur simultaneously. The ratio of CO formation to methane consumption is 0.22, which is associated with reaction rates of steps R4 and R5. This slope is similar to that in Figure 5b, indicating that even under integral reaction conditions for guaiacol, steps R4 and R5 occur essentially as differential reactions.

DOI: 10.1021/acssuschemeng.8b04925
ACS Sustainable Chem. Eng. 2018, 6, 17368−17375

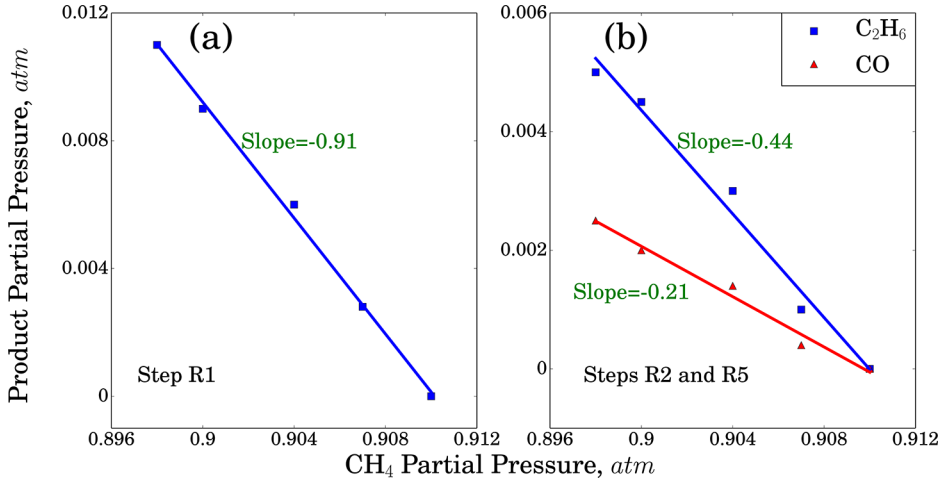


Figure 5. Correlation of methane and gas-phase product partial pressure changes under differential operating conditions over the 5% Pt and 1% Bi catalyst for (a) step R1 (guaiacol to catechol) and (b) steps R2 (catechol to phenol) and R5 (catechol to cyclopentanone). Different methane conversion values, corresponding to different methane and ethane/CO partial pressure changes, were obtained by varying amounts of packed catalyst, while keeping the same feed flow rates/partial pressures of both guaiacol and methane.

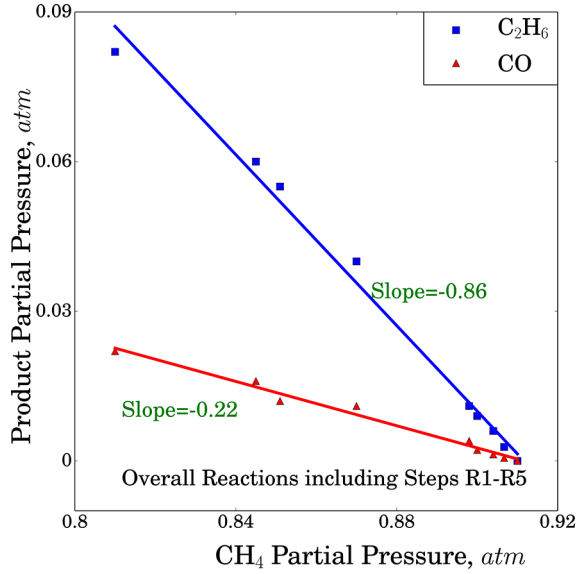


Figure 6. Correlation of methane and gas-phase product partial pressure changes under integral operating conditions over the 5% Pt and 1% Bi catalyst. All five steps (R1−R5) in Figure 4 are continued. Different methane conversion values, corresponding to different methane and ethane/CO partial pressure changes, were obtained by varying amounts of packed catalyst, while keeping the same feed flow rates/partial pressures of both guaiacol and methane.

$^{13}CH_4$ isotopic labeling experiments were also carried out under integral operating conditions over the 5% Pt−1% Bi as well as other catalysts. As shown in Table 4, Bi addition does not significantly affect isotopic distributions of ethane and CO. Over all four catalysts, both $^{12}CH_3-^{13}CH_3$ (about 75−80%) and $^{13}CH_3-^{13}CH_3$ (about 20−25%) were detected in the gas phase by mass spectra, while $^{12}CH_3-^{12}CH_3$ was negligible (<0.02%). Regarding CO, negligible ^{13}CO was detected, implying that the CO product was essentially from guaiacol, including intermediates from it such as catechol, and not methane. The liquid products were also analyzed by GC-MS, and it was found that ^{13}C was not present in any liquid product, thus methane was involved only in forming gas phase products. In addition, the mass balance of ^{13}C atoms was 97 ± 1%, indicating reliable carbon source analysis.

These experimental observations suggest that ethane is formed partially from methane coupling (20−25%), resulting in $^{13}CH_3-^{13}CH_3$, and partially from one methane molecule combining with methyl from guaiacol (75−80%), leading to $^{12}CH_3-^{13}CH_3$. As shown in Figure S5, under nonoxidative conditions, methane coupling to ethane is thermodynamically unfavorable (methane equilibrium conversion <1% when temperature <500 °C).[20] When guaiacol, an oxygenated hydrocarbon, is cofed with methane, steps R1−R4 in Figure 4 are thermodynamically favorable (methane equilibrium conversion ∼100%) in the temperature range 100−800 °C, while step R5 is also thermodynamically favorable at operating temperature 400 °C (methane equilibrium conversion ∼70%). The thermodynamic analysis suggests that guaiacol works as a soft oxidant (see the SI—Definition of Soft Oxidant) for oxidative coupling of methane (OCM).[48−50]

CONCLUDING REMARKS

Following our prior works, related to the development of CH_4 as reductant instead of hydrogen for bio-oil model compound guaiacol deoxygenation, a mechanistic study over various Pt−Bi bimetallic catalysts was carried out, focusing on effects

Table 4. Distribution of Ethane and CO Products (mol %) in Integral Reactions (Steps R1−R5)

	ethane			CO	
catalyst	$^{12}CH_3-^{12}CH_3$	$^{12}CH_3-^{13}CH_3$	$^{13}CH_3-^{13}CH_3$	^{12}CO	^{13}CO
5% Pt	0.0001	0.7721	0.2278	0.9912	0.0088
5% Pt−1% Bi	0.0001	0.7656	0.2343	0.9834	0.0166
5% Pt−2.5% Bi	0.0001	0.7924	0.2075	0.9897	0.0103
5% Pt−5% Bi	0.0002	0.8094	0.1904	0.9909	0.0091

DOI: 10.1021/acssuschemeng.8b04925
ACS Sustainable Chem. Eng. 2018, 6, 17368−17375

of methane/guaiacol feed ratio, Bi loading and the origin of carbon atom source in the gas-phase products: ethane and CO. It was found that excess methane feed favors high guaiacol conversion, and Bi loading amount does not significantly affect product distribution of guaiacol deoxygenation, although Bi addition improves catalyst stability via functioning as site blocker over Pt surface. Utilizing differential and integral reaction observations, isotopic labeling tests reveal that the coproduced ethane is formed from two sources: coupling of two methane molecules (20−25%) facilitated by guaiacol as soft oxidant and a methane molecule combining with a methyl from guaiacol (75−80%), while all CO is formed from guaiacol. The present work provides priciples for operating condition selection and catalyst design for a potential industrial technique that coproduces upgraded bio-oil and ethane, which are derived from lignin fast pyrolysis and shale/natural gas via methane utilization, respectively.

■ ASSOCIATED CONTENT

Supporting Information

The Supporting Information is available free of charge on the ACS Publications website at DOI: 10.1021/acssuschemeng.8b04925.

Materials and catalyst preparation, catalyst characterization, product analysis, definition of soft oxidant, Table S1, and Figures S1−S5 (PDF)

■ AUTHOR INFORMATION

Corresponding Author

*E-mail: avarma@purdue.edu. Phone: 765-494-8484. Fax: 765-494-0805.

ORCID

Yang Xiao: 0000-0003-1705-2213

Arvind Varma: 0000-0002-3472-5929

Notes

The authors declare no competing financial interest.

■ ACKNOWLEDGMENTS

This work was supported by the R. Games Slayter fund and the William and Cynthia Smith gift funds.

■ REFERENCES

(1) Kruse, A.; Funke, A.; Titirici, M. M. Hydrothermal Conversion of Biomass to Fuels and Energetic Materials. *Curr. Opin. Chem. Biol.* **2013**, *17* (3), 515−521.

(2) Sheldon, R. A. Green and Sustainable Manufacture of Chemicals from Biomass: State of the Art. *Green Chem.* **2014**, *16*, 950−963.

(3) Xie, S.; Sun, Q.; Pu, Y.; Lin, F.; Sun, S.; Wang, X.; Ragauskas, A. J.; Yuan, J. S. Advanced Chemical Design for Efficient Lignin Bioconversion. *ACS Sustainable Chem. Eng.* **2017**, *5* (3), 2215−2223.

(4) Sluiter, J. B.; Ruiz, R. O.; Scarlata, C. J.; Sluiter, A. D.; Templeton, D. W. Compositional Analysis of Lignocellulosic Feedstocks. 1. Review and Description of Methods. *J. Agric. Food Chem.* **2010**, *58* (16), 9043−9053.

(5) Mihalcik, D. J.; Mullen, C. A.; Boateng, A. A. Screening Acidic Zeolites for Catalytic Fast Pyrolysis of Biomass and Its Components. *J. Anal. Appl. Pyrolysis* **2011**, *92* (1), 224−232.

(6) Bai, X.; Kim, K. H.; Brown, R. C.; Dalluge, E.; Hutchinson, C.; Lee, Y. J.; Dalluge, D. Formation of Phenolic Oligomers During Fast Pyrolysis of Lignin. *Fuel* **2014**, *128*, 170−179.

(7) Graca, I.; Lopes, J. M.; Cerqueira, H. S.; Ribeiro, M. F. Bio-oils Upgrading for Second Generation Biofuels. *Ind. Eng. Chem. Res.* **2013**, *52* (1), 275−287.

(8) Saidi, M.; Samimi, F.; Karimipourfard, D.; Nimmanwudipong, T.; Gates, B. C.; Rahimpour, M. R. Upgrading of Lignin-derived Bio-oils by Catalytic Hydrodeoxygenation. *Energy Environ. Sci.* **2014**, *7*, 103−129.

(9) DeWild, P. J.; Huijgen, W. J. J.; Gosselink, R. J. Lignin Pyrolysis for Profitable Lignocellulosic Biorefineries. *Biofuels, Bioprod. Biorefin.* **2014**, *8* (5), 645−657.

(10) Hilbers, T. J.; Wang, Z.; Pecha, B.; Westerhof, R. J.; Kersten, S. R.; Pelaez-Samaniego, M. R.; Garcia-Perez, M. Cellulose-Lignin Interactions During Slow and Fast Pyrolysis. *J. Anal. Appl. Pyrolysis* **2015**, *114*, 197−207.

(11) Fan, L.; Zhang, Y.; Liu, S.; Zhou, N.; Chen, P.; Cheng, Y.; Addy, M.; Lu, Q.; Omar, M. M.; Liu, Y.; Wang, Y.; Dai, L.; Anderson, E.; Peng, P.; Lei, H.; Ruan, R. Bio-oil from Fast Pyrolysis of Lignin: Effects of Process and Upgrading Parameters. *Bioresour. Technol.* **2017**, *241*, 1118−1126.

(12) Mortensen, P. M.; Grunwaldt, J. D.; Jensen, P. A.; Jensen, A. D. Screening of Catalysts for Hydrodeoxygenation of Phenol as a Model Compound for Bio-oil. *ACS Catal.* **2013**, *3* (8), 1774−1785.

(13) Ly, H. V.; Im, K.; Go, Y.; Galiwango, E.; Kim, S. S.; Kim, J.; Choi, J. H.; Woo, H. C. Spray Pyrolysis Synthesis of γ-Al_2O_3 Supported Metal and Metal Phosphide Catalysts and Their Activity in the Hydrodeoxygenation of a Bio-Oil Model Compound. *Energy Convers. Manage.* **2016**, *127*, 545−553.

(14) Kay Lup, A. N.; Abnisa, F.; Daud, W. M. A. W.; Aroua, M. K. A Review on Reaction Mechanisms of Metal-Catalyzed Deoxygenation Process in Bio-Oil Model Compounds. *Appl. Catal., A* **2017**, *541*, 87−106.

(15) Cueto-Felgueroso, L.; Juanes, R. Forecasting Long-Term Gas Production from Shale. *Proc. Natl. Acad. Sci. U. S. A.* **2013**, *110* (49), 19660−19661.

(16) Schout, G.; Hartog, N.; Hassanizadeh, S. M.; Griffioen, J. Impact of an Historic Underground Gas Well Blowout on the Current Methane Chemistry in a Shallow Groundwater System. *Proc. Natl. Acad. Sci. U. S. A.* **2018**, *115* (2), 296−301.

(17) Schwach, P.; Pan, X.; Bao, X. Direct Conversion of Methane to Value-Added Chemicals over Heterogeneous Catalysts: Challenges and Prospects. *Chem. Rev.* **2017**, *117* (13), 8497−8520.

(18) Wang, L.; Tao, L.; Xie, M.; Xu, G.; Huang, J.; Xu, Y. Dehydrogenation and Aromatization of Methane under Non-oxidizing Conditions. *Catal. Lett.* **1993**, *21* (1), 35−41.

(19) Lacheen, H. S.; Iglesia, E. Stability, Structure, and Oxidation State of Mo/H-ZSM-5 Catalysts During Reactions of CH_4 and CH_4-CO_2 Mixtures. *J. Catal.* **2005**, *230* (1), 173−185.

(20) Xiao, Y.; Varma, A. Highly Selective Nonoxidative Coupling of Methane over Pt-Bi Bimetallic Catalysts. *ACS Catal.* **2018**, *8* (4), 2735−2740.

(21) Spivey, J. J.; Hutchings, G. Catalytic Aromatization of Methane. *Chem. Soc. Rev.* **2014**, *43* (3), 792−803.

(22) Xiao, Y.; Varma, A. Catalytic Deoxygenation of Guaiacol Using Methane. *ACS Sustainable Chem. Eng.* **2015**, *3* (11), 2606−2610.

(23) Gobolos, S.; Moger, D.; Szabo, S.; Nagy, F. N-Pentane Isomerization in a Continuous-Flow Reactor on Pt/Al_2O_3 Catalysts Modified by Adsorbed Bismuth and Palladium. *React. Kinet. Catal. Lett.* **1980**, *15* (2), 227−232.

(24) Kimura, H.; Tsuto, K.; Wakisaka, T.; Kazumi, Y.; Inaya, Y. Selective Oxidation of Glycerol on a Platinum-Bismuth Catalyst. *Appl. Catal., A* **1993**, *96* (2), 217−228.

(25) Xiao, Y.; Greeley, J.; Varma, A.; Zhao, Z. J.; Xiao, G. An Experimental and Theoretical Study of Glycerol Oxidation to 1,3-Dihydroxyacetone over Bimetallic Pt-Bi Catalysts. *AIChE J.* **2017**, *63* (2), 705−715.

(26) Olcese, R.; Bettahar, M.; Petitjean, D.; Malaman, B.; Giovanella, F.; Dufour, A. Gas-phase Hydrodeoxygenation of Guaiacol Over Fe/SiO_2 Catalyst. *Appl. Catal., B* **2012**, *115−116*, 63−73.

(27) Thangalazhy-Gopakumar, S.; Adhikari, S.; Gupta, R. B.; Fernando, S. D. Influence of Pyrolysis Operating Conditions on Bio-Oil Components: a Microscale Study in a Pyroprobe. *Energy Fuels* **2011**, *25* (3), 1191−1199.

(28) Ruiz, P.; Leiva, K.; Garcia, R.; Reyes, P.; Fierro, J.; Escalona, N. Relevance of Sulfiding Pretreatment on the Performance of Re/ZrO_2 and Re/ZrO_2-sulfated Catalysts for the Hydrodeoxygenation of Guayacol. *Appl. Catal., A* **2010**, *384* (1), 78−83.
(29) Xiao, Y.; Varma, A. Kinetics of Guaiacol Deoxygenation Using Methane over the Pt-Bi Catalyst. *Reaction Chemistry & Engineering* **2017**, *2* (1), 36−43.
(30) Gunawardena, D. A.; Fernando, S. D. Reaction Kinetics of and Coking Behavior During Furan Deoxygenation Via Catalytic Pyrolysis in the Presence of Methane. *Chem. Eng. Technol.* **2017**, *40*, 1176−1183.
(31) Gunawardena, D. A.; Fernando, S. D. Screening of Transition Metal/Oxide-Impregnated ZSM-5 Catalysts for Deoxygenation of Biomass Oxygenates Via Direct Methane Intervention. *Biofuels* **2018**, *9* (1), 113−120.
(32) He, P.; Shan, W.; Xiao, Y.; Song, H. Performance of Zn/ZSM-5 for in Situ Catalytic Upgrading of Pyrolysis Bio-oil by Methane. *Top. Catal.* **2016**, *59* (1), 86−93.
(33) Gao, D.; Schweitzer, C.; Hwang, H. T.; Varma, A. Conversion of Guaiacol on Noble Metal Catalysts: Reaction Performance and Deactivation Studies. *Ind. Eng. Chem. Res.* **2014**, *53* (49), 18658−18667.
(34) Chang, J.; Danuthai, T.; Dewiyanti, S.; Wang, C.; Borgna, A. Hydrodeoxygenation of Guaiacol over Carbon-supported Metal Catalysts. *ChemCatChem* **2013**, *5* (10), 3041−3049.
(35) Jongerius, A. L.; Bruijnincx, P. C. A.; Weckhuysen, B. M. Liquid-phase Reforming and Hydrodeoxygenation as a Two-step Route to Aromatics from Lignin. *Green Chem.* **2013**, *15* (11), 3049−3056.
(36) Hu, W.; Knight, D.; Lowry, B.; Varma, A. Selective Oxidation of Glycerol to Dihydroxyacetone over Pt-Bi/C Catalyst: Optimization of Catalyst and Reaction Conditions. *Ind. Eng. Chem. Res.* **2010**, *49* (21), 10876−10882.
(37) Sethia, G.; Sayari, A. Activated Carbon with Optimum Pore Size Distribution for Hydrogen Storage. *Carbon* **2016**, *99*, 289−294.
(38) Antolini, E.; Salgado, J. R.; Gonzalez, E. R. The Stability of Pt-M (M = First Row Transition Metal) Alloy Catalysts and Its Effect on the Activity in Low Temperature Fuel Cells: a Literature Review and Tests on a Pt-Co Catalyst. *J. Power Sources* **2006**, *160* (2), 957−968.
(39) Fischer, C.; Thede, R.; Baumann, W.; Drexler, H. J.; Konig, A.; Heller, D. Investigations Into Metal Leaching from Polystyrene-Supported Rhodium Catalysts. *ChemCatChem* **2016**, *8* (2), 352−356.
(40) Xiao, Y.; Varma, A. Conversion of Glycerol to Hydrocarbon Fuels via Bifunctional Catalysts. *ACS Energy Letters* **2016**, *1* (5), 963−968.
(41) Zhu, Z.; Lu, G.; Guo, Y.; Guo, Y.; Zhang, Z.; Wang, Y.; Gong, X. Q. High Performance and Stability of the Pt-W/ZSM-5 Catalyst for the Total Oxidation of Propane: the Role of Tungsten. *ChemCatChem* **2013**, *5* (8), 2495−2503.
(42) Wu, Z.; Wegener, E. C.; Tseng, H. T.; Gallagher, J. R.; Harris, J. W.; Diaz, R. E.; Ren, Y.; Ribeiro, F. H.; Miller, J. T. Pd-In Intermetallic Alloy Nanoparticles: Highly Selective Ethane Dehydrogenation Catalysts. *Catal. Sci. Technol.* **2016**, *6*, 6965−6976.
(43) Bergeret, G.; Gallezot, P. Particle Size and Dispersion Measurements. *Handbook Hetero. Catal.* **2008**, *1*, 738−765.
(44) Figueiredo, M. C.; Melander, M.; Solla-Gullon, J.; Kallio, T.; Laasonen, K. Bismuth and CO Coadsorption on Platinum Nanoparticles. *J. Phys. Chem. C* **2014**, *118* (40), 23100−23110.
(45) Paffett, M. T.; Campbell, C. T.; Windham, R. G.; Koel, B. E. A Multitechnique Surface Analysis Study of the Adsorption of H_2, CO and O_2 on BiPt(111) Surfaces. *Surf. Sci.* **1989**, *207* (2), 274−296.
(46) Pasti, I.; Mentus, S. DFT Study of Adsorption of Hydrogen and Carbon Monoxide on Pt_xBi_{1-x}/Pt(111) Bimetallic Overlayers: Correlation to Surface Electronic Properties. *Phys. Chem. Chem. Phys.* **2009**, *11*, 6225−6233.
(47) Gao, D.; Xiao, Y.; Varma, A. Guaiacol Hydrodeoxygenation over Platinum Catalyst: Reaction Pathways and Kinetics. *Ind. Eng. Chem. Res.* **2015**, *54* (43), 10638−10644.
(48) Voskresenskaya, E.; Kurteeva, L.; Pervyshina, G.; Anshits, A. Comparison of O_2 and N_2O as Oxidants for the Oxidative Coupling of Methane over Bi-containing Oxide Catalysts. *Catal. Today* **1995**, *24* (3), 277−279.
(49) Al Mayman, S.; Zeghayer, Y. A.; Al Masry, I. A.; Ramay, S.; Jbar, A.; Al Nashef, I. Study of Performance of CeO_2/ZnO Nanocatalysts for the Oxidative Coupling of Methane using Carbon Dioxide as Oxidant. *Int. J. Phys. Sci.* **2012**, *7* (1), 6270−7279.
(50) Peter, M.; Marks, T. J. Platinum Metal-Free Catalysts for Selective Soft Oxidative Methane to Ethylene Coupling. Scope and Mechanistic Observations. *J. Am. Chem. Soc.* **2015**, *137* (48), 15234−15240.

DOI: 10.1021/acssuschemeng.8b04925
ACS Sustainable Chem. Eng. 2018, 6, 17368−17375